

Synthesis and characterization of high luminescent zinc sulphide

Nanoparticles by a novel single source precursor route.

*Arvind Kumar^a, Upendra K. Tripathi^b, D. Kumar^a, Rayees A. Bhat^c

^a Centre of Research for Chemical Sciences, Govt. Model Science College,

Jiwaji University Gwalior, M.P. - 474009 India.

^b Department of Chemistry, Janta Mahavidyalaya Ajitmal, Auraiya-206121(C.S.J.M.

University, Kanpur, U.P.) India

^c Department of Chemistry, Babasaheb Bhimrao Ambedkar University (A Central University),

Lucknow-226025, U.P., India

Corresponding Autor : Arvind Kumar

Abstract :

In the present work, we have reported microwave assisted synthesis of highly luminescent zinc sulphide (ZnS), nano-particles (NPs) using dithiocarbazate Zn (II) chloride complex single-molecule precursor route. The single source precursor (SSPs) are heated using microwave irradiation to obtain ZnS NPs. The irradiation of precursor in DMSO environment played an important role in reducing reaction time, minimizing possibility of side reactions and resulted in obtaining good quality NPs.

The structure and composition of prepared nanoparticles are characterized by XRD, SEM, TEM, IR and U.V.- Visible spectrophotometry techniques.

Keywords : ZnS; Dithiocarbazate; Nanoparticles; Single molecular precursor; Luuminescent; Microwave oven, stirrer.

1. Introduction :

In recent year's great attraction and interest have been considered for preparation and characterization of Nano sized dimensions and special morphology in material science and

nanotechnology^[1-2]. Zinc Sulfide (ZnS) is a wide band-gap (3.5-3.7 eV) semiconductor the finds use in optoelectronic devices due to its unique photoluminescence and electro-luminescence properties^[3] Nano- dimensional ZnS is especially important as both its optical and electronic properties can be tailored by controlling the size and shape of the nanostructure^[4-7]. More over a variety of methods have been reported to prepare zinc sulphide^[8, 9].

Recently microwave assisted method has drawn much attention in nanoscale synthesis. When compared with the above methods, microwave-assisted method has its own superiority.

An interesting feature of semiconductor materials is that they can be prepared in a few nano meter-sized crystals, which have physical and chemical properties that are different from those of crystals with 'bulky' structure. Most of the physical and chemical properties are controlled by the particle size (Attanavake et al., 2020) . However, by bringing the size down to the nanometre scale, a large number of atoms on the particle surface are then less coordinated, so making the particles thermodynamically unstable. The less coordinated atoms readily chelate with ligands or surfactants (Yang et al., 2014). Among semiconductor nanocrystals, ZnS nanoparticles (NPs) are of interest due to their fascinating crystalline structures. It is well known that ZnS NPs may exist in cubic phase (zincblende) at room temperature with a bandgap of 3.68 eV, which converts to hexagonal phase (wurtzite) at higher temperatures with a bandgap of 3.77 eV (Tiwari and Dhoble., 2016). Based on the wide bandgap, ZnS NPs have the potential to be utilized in a wide range of applications in photonics, electronics, solar cells, and LEDs (Niu et al., 2014). The single molecule precursors were synthesized by Schiff bases derived from S-alkyl/aryl esters of dithiocarbazic acid^[10-12] and their physico chemical properties^[13, 14], biological activities^[15, 16] were studied.

In the present work, ZnS-nano particles are obtained by micro wave assisted method using dithiocarbazate ligand as a single molecular precursor and their optical, morphological and structural characterization is studied.

2. Experimental :

2.1-Materials used :

Analytical grade chemicals and reagent, Potassium hydroxide (KOH), zinc acetate, hydrazine hydrate, carbon disulphide, ethanol, dimethyl sulfoxide (DMSO) methyl iodide, and 3,5-dibromo-4-hydroxy benzaldehyde of Ranbaxy are used throughout the work.

2.2-Instruments used :

Electrical stirrer, water bath, ultrasonicator, microwave oven.

2.3-Synthesis of ZnS nanoparticles :

All process of synthesis is carried out into three parts-

- Synthesis of s- methyl dithiocarbazate (SMDTC) ligand.
- Synthesis of Schiff base of SMDTC ligand and metal complex.
- Synthesis of nanoparticles

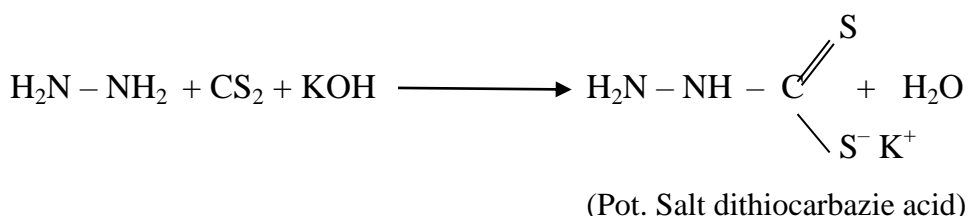
2.3.1-Synthesis of s- methyl dithiocarbazate (SMDTC) ligand :

The process of synthesis of s-methyl dithiocarbazate ligand can further be divided into two step

Step-1

Synthesis of potassium salt of dithiocarbazic acid

Initially ethanol and distilled water is added in the ratio 9:1 and shaken well so that a 70 ml solution is formed. Now potassium hydroxide 11.4 g (0.2mol) was added and stirred well. This mixture was cooled in ice temperature. Hydrazine hydrate 10 g (0.2 mol) was added in the cooled solution slowly with constant stirring.



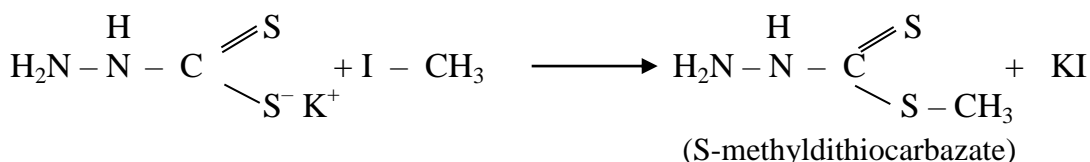
(Reaction-1)

Another solution of carbon disulfide CS₂ 15.2g (0.2 mol) is prepared by adding it in ethanol (12.5ml). Solution of CS₂ was added dropwise from dropping funnel into cooled solution of hydrazine hydrate and KOH with constant stirring upto an hour and then kept the mixture in inert medium. Two layers are observed after another 15-20 minutes. The yellow oily layer was then separated using a separating funnel and dissolved in previously cooled 40% ethanol (30ml). The mixture was kept in ice bath. Structure of potassium salt of dithiocarbazic acid is shown in reaction-1.

Step-2

The synthesis of s-methyl dithiocarbazate ligand

The synthesis of s-methyl dithiocarbazate ligand and Schiff base have already been reported^[18]. In this process methyl iodide (10ml) was added slowly in mixture with vigorous mechanical stirring upto 30 minutes. White product was obtained and stirring was continued for another 10 minutes till the product separated out. Structure of S-methyl dithiocarbazate is shown in reaction-2.



Reaction-2

The product was filtered off, washed with water, and then dried in air. The crude product was recrystallized from ethanol and dried in vacuum desiccator over P₂O₅. The yield was calculated by weighing method and found to 40%. The melting point measured is 126°C.

2.3.2 - Synthesis of Schiff base of SMDTC ligand and its metal complex :

Firstly, S-methyl dithiocarbazate (0.022 mole, 2.44g) was dissolved in ethanol (30-40 ml) at temperature 40^oc, then an equimolar amount (0.02mol5.082 g) of 5-bromo-2-hydroxy-3-methoxy benzaldehyde was added in absolute ethanol (30ml) in separate flask. Finally, both the solution were added and the mixture was heated at 60^oc for 5 hours and cooled to 0^oC in an ice bath. The product was filtered, washed with absolute ethanol, recrystallized from absolute ethanol and dried over silica gel. Now prepared Schiff base 5-bromo-2-hydroxy-3-methoxy benzaldehyde of SMDTC (1mM) was dissolved in ethanol (30 ml), and this mixture was added gradually to the ethanolic solution of zinc acetate which was prepared by dissolving (0.5mM) of salt in 25ml of ethanol with continuous stirring. Yellow solid precipitate of Zn complex so formed was filtered off and washed thoroughly with ethanol.

2.3.3-Synthesis of nanoparticles :

Ultrasonication : For obtaining ZnS nanoparticles, 1g of the zinc complex was dissolved in 25ml DMSO in a round bottom flask. A ultrasonic treatment (using piezoelectric sandwich transducer at 40 kHz resonant frequency) was given for 30 minutes at 78^oc to it thoroughly and then kept for 35 minutes.

Microwave irradiation: Final product was heated in microwave oven for 10 minutes with 800 W power microwave treatment resulted suddenly formation of ZnS nanoparticles. The solution containing nanoparticles was then cooled, centrifuged and washed with absolute methanol several times.

3. Characterization :

ZnS-NP are characterized by structural, morphological and optical study. Powder X-ray diffraction pattern is obtained by X Pert Pro PAN analytical X-ray diffractometer in the 2 θ ranging from 20 to 80^oC with CuK α radiation of wavelength 1.54 Å⁰. TEM and HRTEM micrographs are obtained by TECHAI G2F20 operated at 300 KV using a drop of suspension of the sample in ethanol on carbon coated copper grid. Optical spectra of the ZnS structures on quartz in the range 200-900 nm is obtained using Perkin Elmer Lambda 25 spectrophotometer. Photoluminescence spectrum is obtain using Perkin Elmer PL-55 with exciton at 300 nm.

4. Results and Discussion :

Yellow colour ZnS nanoparticles is obtained within a short reaction time using microwave heating in DMSO. Microwave irradiated material are of high quality as microwave irradiation provides selective rapid uniform heating high reaction rate, and low-energy consumption. It also helps to deliver energy into the reaction vessel and accelerates the reaction speed and efficiency. The microwave heating reduced the crystallization time and improved the crystallinity of the final product in a specific way. In our case, it helps to obtain good quality nanorods. The DMSO solvent also plays a very important role in nanorod synthesis. DMSO has very high (0.825) value of loss tangent ($\tan \delta$) and hence efficiently convert electromagnetic energy into heat at a given frequency. DMSO having high boiling point and high permanent dipole is an excellent absorber of the microwave irradiation, which can take up the energy from the microwave field and get the polar reaction solution heated up to high temperature instantaneously^[19,20]. The polar solvent acting both reaction media and dispersion media can efficiently absorb and stabilize the surface of the particles and produce monodispersed ZnS nanoparticles^[21]. The short reduction time results in increasing product purities by reducing unwanted side reactions compared to conventional heating methods. Microwave reactors allow easy access to high temperature and pressures. Structural, morphological, and optical studies were performed on the samples

4.1- X-ray diffraction analysis of zinc sulfide :

The analysis of x-ray pattern (Fig. 1) shows that ZnS sample crystallize in cubic symmetry ($F-43M$ space group) with lattice parameter $a = 5.368(4) \text{ \AA}$ and unit cell volume $V = 154.7157(8) \text{ \AA}^3$. The three different peaks of the sample correspond to the lattice planes of (111), (220), and (311), which match very well with the cubic zinc blende structure.

The significant broadening of the XRD pattern peaks reveals the small particle (crystallite) size and indicates the Nano metric particle size. The average particle size is approximately estimated by Hall's method

$$\frac{\beta \cos \theta}{\lambda} = \frac{1}{D} + \frac{2\epsilon \sin \theta}{\lambda}$$

here β is the full width at half maximum (FWHM) of that peak in radian, θ is the diffraction angle of the Bragg peak, $\lambda = 1.54056 \text{ \AA}$ is the wavelength of the used x-ray, D is the particle size, and ε is the effective residual strain. In this way, D and ε can be estimated from the intercept on the $\beta \cos \theta / \lambda$ axis and the slope of the curve by plotting the $\beta \cos \theta / \lambda$ versus $\sin \theta / \lambda$, respectively. An average particle size of about 5.5 nm is obtained.

A dislocation is a crystallographic defect that strongly affects many properties of zinc sulphide, so the dislocation density is also calculated from the following relation:

$$\delta = \frac{15\varepsilon}{aD} \quad (2)$$

The effective strain and also the dislocation density are estimated to be 6.71×10^{-3} and 3.41×10^{15} , respectively.

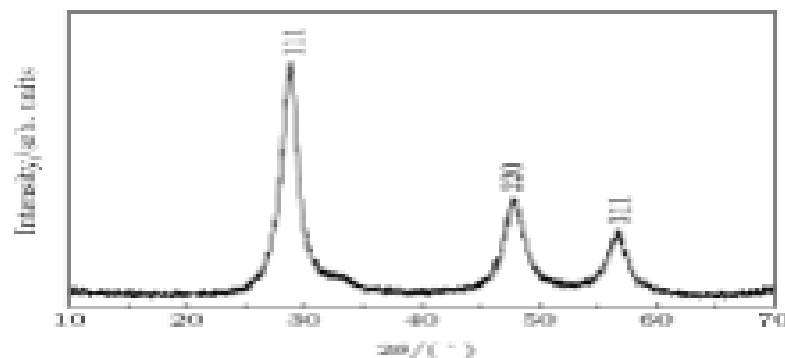


Fig-1. X-ray diffraction for ZnS nanoparticles

4.2-Scanning electron microscopy

The SEM image of ZnS nanoparticles is shown in Fig. 2. The SEM microstructural analysis shows that the synthesized ZnS contains mainly the grains of ZnS particles (crystallite) with regular shape. One can see that nearly spherical nanoparticles have an almost homogenous size distribution with a mean size of 50 nm. In the absence of EDTA, a bulk ZnS sample is formed (not shown here). In the synthesis process, the usage of EDTA causes the stabilization of the small particles and the inhibition of this agglomeration. Due to

the existence of – COOH group in EDTA molecules which absorbed on the particle surface, EDTA-capped ZnS sample is formed. The maximum particle size does not exceed 70 nm.

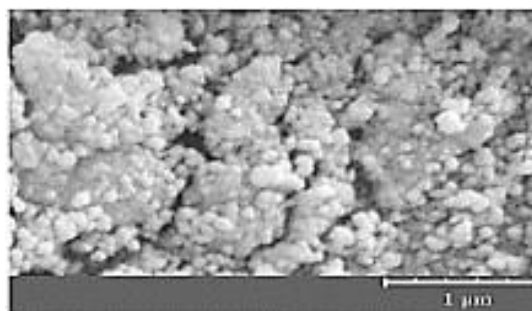


Fig. 2. SEM image of ZnS nanoparticles

4.3-Transmission electron microscopy

The TEM image of zinc sulphide is shown in figure 3 which shows spherical particles agglomerated with size 7.8 nm. The size of particles observed in the TEM micrograph is larger than that of the crystallites estimated from the Debye-Scherrer equation. We think that each particle consists of fine crystallites whose sizes were determined by the XRD technique. Thus each particle in the TEM micrograph was found polycrystalline.

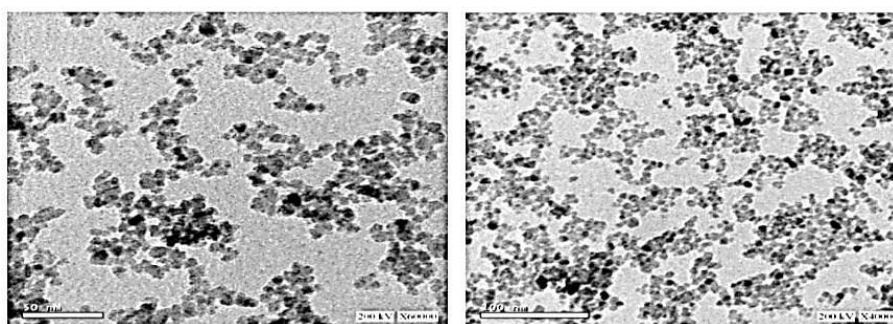


Fig-3. TEM image of ZnS nanoparticles

4.4- Fourier Transforms infrared measurement

The FTIR spectrum of ZnS nanoparticles at room temperature is shown in Fig. 3. This spectrum shows the IR absorption due to the various vibration modes. The characteristic major peaks of ZnS can be observed at about 1124, 998, and 624 cm^{-1} , which are in good agreement with the reported results. The observed peaks at 1550 cm^{-1} – 1750

cm^{-1} are assigned to the C = O stretching modes, and also the broad absorption peaks in a range of $3100 \text{ cm}^{-1} - 3600 \text{ cm}^{-1}$ correspond to O-H stretching modes arising from the absorption of water on the surface of nanoparticles via -COOH group.

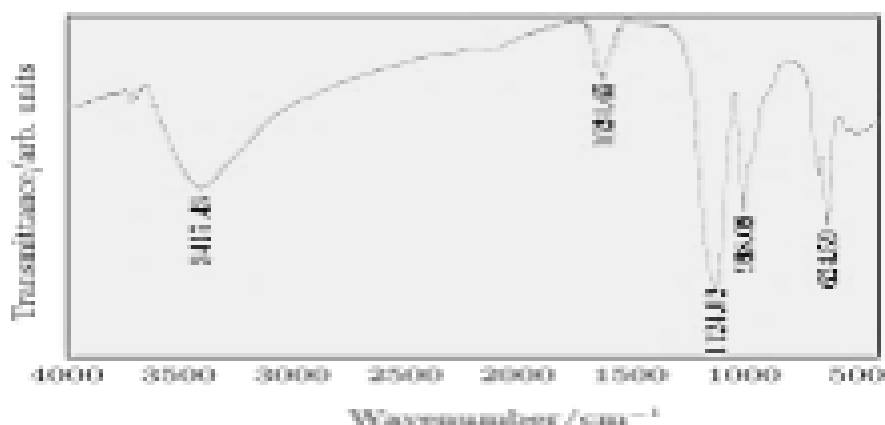


Fig-3. FTIR spectrum of zinc sulphide nanoparticles

4.5- U.V-visible spectrum

At room temperature UV-Visible spectrum in the absorption mode is measured and shown in Fig. 4. As can be seen, the strongest excitonic absorption peak of the synthesized ZnS nanoparticles appears at around 303 nm. The optical band gap of the nanoparticles is calculated from the UV absorption study, which corresponds to the transition from the valance band to the conduction band, using the following equation

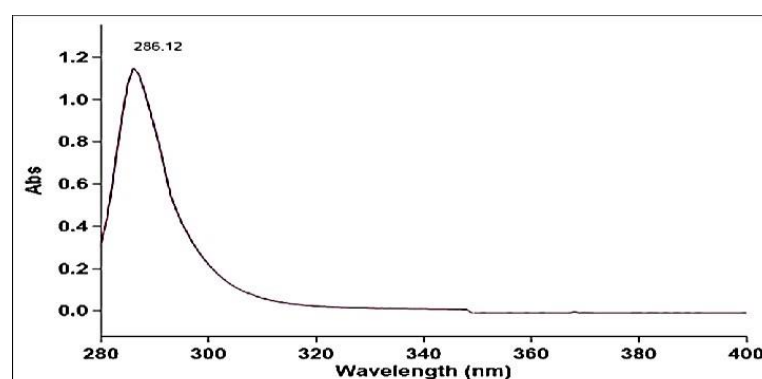


Fig4. U.V- visible spectrum of ZnS nanoparticles

$$\alpha h\nu = A(h\nu - E_g^{opt})^n \quad - \quad (3)$$

where α is the absorption coefficient, $h\nu$ is the incident photon energy, A is a constant, and E_g^{opt} is the optical band gap energy of the material. The value of the exponent depends on the type of transition: 1/2 for allowed direct transition and 2 for allowed indirect transition. The optical band gap of ZnS nanoparticles is determined by plotting $(\alpha h\nu)^2$ versus $h\nu$ and extrapolating the straight line portion of $(\alpha h\nu)^2$ to $(\alpha h\nu)^2 = 0$ (Fig. 4).

The value of the optical band gap energy is found to be 4.03 eV (the inset in Fig. 4). A comparison with the value of bulk ZnS of 337 nm (3.68 eV) shows that the band edge is blue-shifted. The absorption spectrum of ZnS nanoparticle shifts towards the lower wavelength side, which can be explained as being due to the quantum size effect. Due to the quantum confinement effect of semiconductor nanoparticles in their electronic structure, which originates from the electron-hole confinement in a small volume, the increasing band gap energy occurred.

The particle size is also calculated from the absorption data using the effective mass approximation relation as follows :

$$E_g^{opt} = E_g + \frac{h^2}{8r^2} \left(\frac{1}{m_e^*} + \frac{1}{m_h^*} \right) - \frac{1.8e^2}{4\pi\epsilon\epsilon_0 r} \quad (4)$$

where E_g is the calculated optical band gap of the nanoparticles and the bulk band gap (ZnS = 3.68 eV) in J , respectively, h is Planck's constant, r is the radius of the nanoparticle in meter, m_e^* and m_h^* are the electron and hole effective mass, e is the charge of the electron in C , ϵ is the dielectric constant (ZnS = 8.3), and ϵ_0 is vacuum permittivity constant in $C^2 \cdot J^{-2} \cdot M^{-1}$. The calculated particle size is about 3.6 nm, which is in agreement with the size estimated from the XRD result, approximately.

4.6-Photoluminescence spectrum of ZnS nanoparticles

Figure-5 shows the photoluminescence spectrum of as-synthesized ZnS nanoparticles to investigate luminescence properties. Pure ZnS in the form of bulk and nano-crystals shows a main well-known emission band, which is the blue band. Vacancies of sulfur and zinc are equivalent to localized donor and acceptor states, respectively. Owing to these two levels in the energy gap, two optical transitions in the observed UV range can occur. For the pure

sample (Fig. 5) two emission peaks are observed at about 430 nm and 442 nm when excited by UV light. These blue fluorescence light emissions are attributed to the recombination from the shallow electron trap states (sulfur-vacancy) to the valence band and conduction band to zinc vacancy trap, respectively.

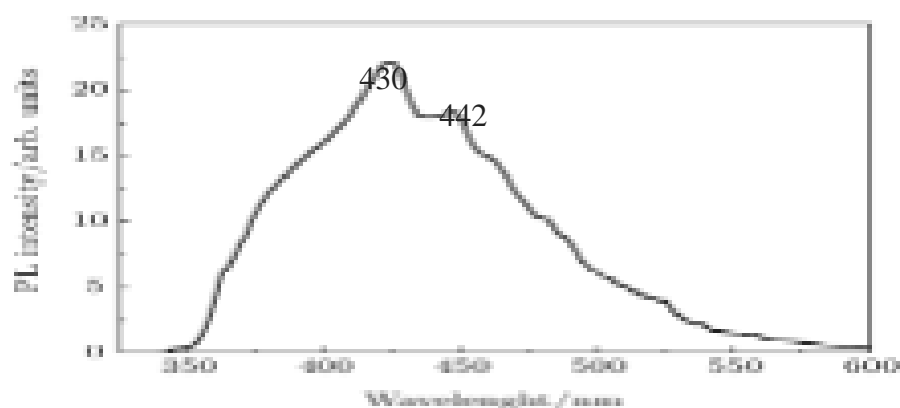


Fig. 5. Room-temperature photoluminescence emission spectrum of ZnS nanoparticles.

5. Conclusions

ZnS nanoparticles are successfully synthesized via using microwave irradiation of dithiocarbamate ligand as a single molecular precursor source. The use of DMSO for microwave irradiation help to decompose precursor very fast in the form of chemical bonding and structural properties of sample are characterized by FTIR and x-ray diffraction to identify the chemical and crystal structure. The x-ray diffraction pattern indicates the cubic zinc-blended structure of ZnS nanocrystals. The SEM image reveals that the ZnS nanoparticles have regular shapes with an average size of 50 nm. TEM images disclose the spherical shape of ZnS nanoparticles with an average particle size is 7.8 nm. The UV spectrum of ZnS nanoparticles shows the strong quantum confinement effect with a blue shift in the band gap energy due to the nanocrystalline ZnS particles. Excellent Photo Luminescence (PL) spectrum consists of 430- and 442-nm emission bands.

6. References :

1. S.M. Pourmortazavi, M.Rahimi-Nasrabadi, A.A.Davoudi-Dehaghani, A. Javidan, M.M. Zahedi, S.S. Hajimirsadeghi : Mater. Res. Bull. 47(2012) 1045-1050.
2. S.M. Pourmortazavi, S.S.Hajimirsadeghi. I.Kohsari, R. Fareghi Alamdari, M. Rahimi-Nasrabadi : Chem. Eng. Technol. 31 (2008) 1532-1535.
3. X. Fang, T. Zhai, U.K. Gautam, L.Li, Wu.Y. Bando, D. Golberg, Prog : Mater. Sci., 2011, 56, 175-287.
4. X. Fang, L.Wu, L.Hu : Adv. Mater, 2011, 23, 585-598.
5. L. W. Yin, Y. Bando, J.H. Zhan, M.S. Li, D. Galberg : Adv. Mater., 2005, 17, 1972-1977.S. Hamad,
6. S.H. Woodley, C.R.A. Catlow, Mol Simulation, 2009, 35, 1015-1032.
7. A. Tiwari, S.J. Dhoble : Cryst Grow. Design, 2017, 17, 381-407.
8. R.F. Zhuo, H.T. Feng, D. Yan, J.T. Chen, J.J. Feng, J.Z. Liu, P.X. Yan : J. Cryst. Growth 310 (2008) 3240-3246.
9. Jiazhao Wang, Guoxiu Wang, Li Yang, Huakum Liu : J Solid State Electrochem (2006) 10: 250–254 DOI 10.1007/s10008-005-0684-4.
10. M.A. Ali, A. H. Mirza, C. W. Voo, A. L. Tan, P. V. Bernhardt : polyhedron. 22 (2003) 3433.
11. M. A. Ali, A. H. Mirza M. Nazimuddin, R. Ahmed, L. R Gahan P. V. Bernhardt : polyhedron 20, (2003) 1479.
12. M.A. Ali, A.H. Mirza, T.W. Keng, R.J. Butcher : Transit Met Chem.28 (2003) 241.
13. D.X. West, S.B. Padhye, P.B. Sonawane : Struct Bond.76 (1991)1.
14. B.A. Hess, J. Schaad, p. Carsky and R. Zahradnik : Chem. Rev., 86 (1986) 709.
15. K. Arora, D. Kumar; Saudi : J. Chem. Soc. 15 (2011) 161.
16. D. Kumar, M.C. Agrawal, R. Singh : Asian J. Chem. 19 (2007) 19.
17. N. Revaprasadu, S.N. Mlondo : Pure Appl. Chem. 78 (2006) 9.
18. L.F. Audrieth, E.S. Scott, P.S. Kippur : J. Org. Chem. 19 (1954) 733.

19. F. Dang, K. Kato, H. Imai, S. Wada, H. Haneda : Ultrasonochem 7(2) (2010) 310-314.
20. W. Tu, H.Liu : Chem Mater. 12(2). (2000) 564-567.
21. C. Feldmann and Christ of Metzmacher : J. Mater. Chem. 11(2001) 2603-2606.